

Circuits and Systems for Receiving, Transmitting and Signal Processing

Устройства и системы передачи, приема и обработки сигналов

Research article

DOI: <https://doi.org/10.18721/JCSTCS.18405>

UDC 621.391.8



LOW COMPUTATIONAL COMPLEXITY TECHNIQUE BASED ON A POLYPHASE STRUCTURE FOR MODULATION AND DEMODULATION OF FBMC/OQAM-OTFS SIGNALS

B.T. Khuc  , A.L. Gelgor

St. Petersburg State Polytechnical University,
St. Petersburg, Russian Federation

 khucbang@mail.ru

Abstract. The paper proposes a low computational complexity technique based on a polyphase structure for modulation and demodulation of FBMC/OQAM-OTFS signals. This approach effectively reduces the overall computational complexity when compared to the frequency spreading approach (FS-FBMC/OQAM-OTFS), which in turn outperforms the direct modulation and demodulation approach for FBMC/OQAM-OTFS signals (Direct-FBMC/OQAM-OTFS). Simulation results explicitly demonstrate that, for an overlapping factor of $K = 4$, various PPN-FBMC/OQAM variants can indeed achieve a 2.5–4 times reduction in the computational complexity with an energy loss of no more than 1 dB compared to FS-FBMC/OQAM-OTFS. These obtained results are observed under standard multipath channel profiles such as EPA, EVA, and ETU in both moderately and highly dynamic scenarios. These findings suggest that the PPN-FBMC/OQAM-OTFS technique is a feasible and promising alternative to conventional OFDM in high-mobility wireless scenarios.

Keywords: OFDM, OTFS, FS-FBMC/OQAM-OTFS, PPN-FBMC/OQAM-OTFS, highly dynamic channel

Citation: Khuc B.T., Gelgor A.L. Low computational complexity technique based on a polyphase structure for modulation and demodulation of FBMC/OQAM-OTFS signals. Computing, Telecommunications and Control, 2025, Vol. 18, No. 4, Pp. 53–66. DOI: 10.18721/JCSTCS.18405



ВЫЧИСЛИТЕЛЬНО ЭФФЕКТИВНЫЙ АЛГОРИТМ НА ОСНОВЕ ПОЛИФАЗНОЙ СТРУКТУРЫ ДЛЯ МОДУЛЯЦИИ И ДЕМОДУЛЯЦИИ СИГНАЛОВ FBMC/OQAM-OTFS

Б.Т. Хук  , А.Л. Гельгор

Санкт Петербургский государственный политехнический университет,
Санкт-Петербург, Российская Федерация

 khucbang@mail.ru

Аннотация. В данной статье предлагается новый и перспективный подход на основе полифазной структуры для вычислительно эффективной модуляции и демодуляции сигналов FBMC/OQAM-OTFS, называемый PPN-FBMC/OQAM-OTFS. Предлагаемый подход обеспечивает снижение вычислительной сложности по сравнению с подходом на основе расширения частоты FS-FBMC/OQAM-OTFS, который, в свою очередь, уже превосходит метод прямой модуляции и демодуляции сигналов FBMC/OQAM-OTFS. Результаты моделирования проведенных исследований наглядно показывают, что при использовании прототипа-фильтра Phydyas с коэффициентом перекрытия $K = 4$ различные варианты PPN-FBMC/OQAM-OTFS действительно могут обеспечить существенный выигрыш в вычислительной сложности в 2,5–4 раза при энергетических потерях не более 1 дБ по сравнению с FS-FBMC/OQAM-OTFS. Эти результаты были получены при стандартных многолучевых каналах, таких как EPA, EVA и ETU как в умеренно-, так в высоко-динамичных сценариях. Полученные результаты позволяют предположить, что технология PPN-FBMC/OQAM-OTFS является работоспособной и перспективной альтернативой традиционному OFDM в условиях беспроводной связи с высокой мобильностью.

Ключевые слова: OFDM, OTFS, FS-FBMC/OQAM-OTFS, PPN-FBMC/OQAM-OTFS, высоко-динамичный канал

Для цитирования: Khuc B.T., Gelgor A.L. Low computational complexity technique based on a polyphase structure for modulation and demodulation of FBMC/OQAM-OTFS signals // Computing, Telecommunications and Control. 2025. T. 18, № 4. C. 53–66. DOI: 10.18721/JCSTCS.18405

Introduction

Currently, more diverse transmission channel conditions have emerged in communication systems including highly dynamic channels due to increased user speeds [1]. This causes the transmission channel to be frequently affected by time and frequency selectivity, resulting from multipath and Doppler effects [2].

In modern communication systems, including 5G New Radio, Orthogonal Frequency Division Multiplexing (OFDM) modulation remains the preferred choice due to its ability to mitigate Inter-Symbol Interference (ISI) and its simplicity in design [3]. However, OFDM modulation suffers severe performance degradation in highly dynamic channels caused by Inter-Carrier Interference (ICI). Additionally, OFDM provides high Out of Band Emission (OOBE) levels due to the use of rectangular pulse for the signal generation and low spectral efficiency due to the use of cyclic prefix [3, 4]. Therefore, in recent works [5, 6], a new modulation technique called FBMC/OQAM-OTFS (Filter-Bank Multi-Carrier with Offset Quadrature Amplitude Modulation and Orthogonal Time-Frequency Space pre-processing) has been proposed to overcome these limitations. This technique has the following advantages:

- 1) it provides low OOB levels due to the use of prototype filter for each subcarrier;
- 2) cyclic prefixes are not required, leading to an increased spectral efficiency;
- 3) its Bit Error Rate (BER) performance doesn't fall, i.e., doesn't saturate, even in highly dynamic wireless channels.

Despite its significant performance advantages, the direct implementation of FBMC/OQAM-OTFS (Direct-FBMC/OQAM-OTFS) faces major limitations in terms of computational complexity. Specifically, it requires extremely high computational demands, as well as substantial processing and latency burdens for the system [6, 7]. The work [7] has shown that the computational cost of the Direct-FBMC/OQAM-OTFS modulation/demodulation scheme can be up to 10^4 times higher than that of conventional OFDM schemes. Therefore, the implementation of Direct-FBMC/OQAM-OTFS in next-generation communication systems is practically infeasible.

A commonly adopted approach for implementing the FBMC/OQAM-OTFS technique is based on frequency spreading (FS) FBMC/OQAM-OTFS. This approach aims to filter the real and imaginary parts of information symbols in the frequency domain by upsampling and filtering before the Inverse Fast Fourier Transform (IFFT) operation with the extended size. The FS-FBMC/OQAM-OTFS allows a reduction of the computational complexity compared to the direct method by up to hundreds of times [7, 8]. However, the computational complexity of the FS-FBMC/OQAM-OTFS technique is still very high compared to the OFDM modulation (about 11–16 times higher) due to the use of the Fast Fourier Transform (FFT)/IFFT blocks of extended-size [4]. As a result, the adaptation of FBMC/OQAM-OTFS in next-generation mobile communication systems continues to face considerable challenges.

In this work, we propose two variants of the FBMC/OQAM-OTFS implementation based on a polyphase network structure (PPN-FBMC/OQAM-OTFS). Unlike the FS-FBMC/OQAM-OTFS approach, in the PPN-FBMC/OQAM-OTFS approach, the filtering process is implemented by the filter bank based on the polyphase structure, similar to how it is done for FBMC/OQAM [7]. The proposed PPN-FBMC/OQAM-OTFS schemes achieve a reduction in computational complexity by a factor of 2.5 to 4, with less than 1 dB energy loss across various multipath channel profiles, compared to FS-FBMC/OQAM-OTFS.

Direct form of FBMC/OQAM-OTFS implementation

Through this paper, we assume that one FBMC/OQAM-OTFS framework has a bandwidth B_w and a period T_{Frame} , in which B_w contains M subcarriers and T_{Frame} is divided into N sub-symbols (i.e., $B_w = M\Delta f$, $T_{\text{Frame}} = NT$). Then, the Doppler and delay steps can be expressed as $1/NT$ and $1/M\Delta f$, respectively. The transformation chain in system using FBMC/OQAM-OTFS is shown in Fig. 1. Fig. 2 shows the Delay-Doppler (DD) grid that is used to map/demap the information symbols in the OTFS Pre/Post-Processing procedure.

In the FBMC/OQAM-OTFS technique, QAM information symbols are first mapped into the DD domain – $x^{\text{DD}}[n, l]$, where $n = 0, \dots, N - 1$, $l = 0, \dots, L - 1$. Then, $x^{\text{DD}}[n, l]$ are converted in the time-frequency (TF) domain $X^{\text{TF}}[m, k]$ by using inverse symplectic FFT (ISFFT) [1]:

$$X^{\text{TF}}[l, k] = \frac{1}{\sqrt{NL}} \sum_{n=0}^{N-1} \sum_{l=0}^{L-1} x^{\text{DD}}[n, l] \exp\left(-j2\pi\left(\frac{nm}{N} - \frac{lk}{K}\right)\right). \quad (1)$$

In an FBMC/OQAM system, OQAM pre-processing is performed in the TF domain by shifting the real and imaginary parts of QAM symbols by half of the symbol period, $T/2$. As a result, after OQAM pre-processing, the symbol count is doubled compared to a conventional OFDM modulation, and the symbol period becomes equal to $T/2$ [5, 6]:

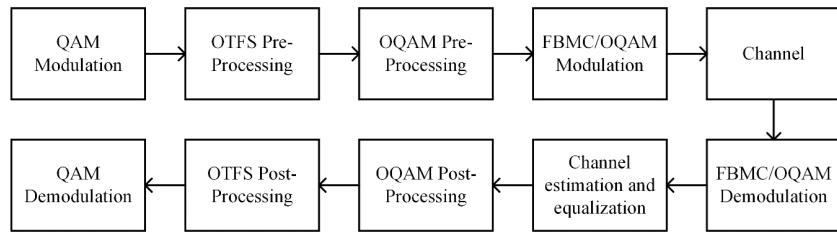


Fig. 1. FBMC/OQAM-OTFS scheme

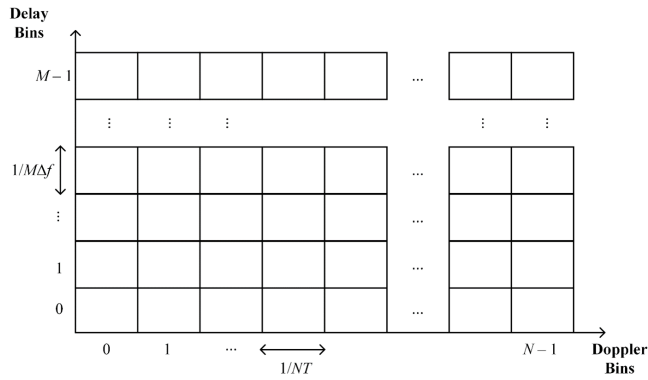


Fig. 2. OTFS DD grid

$$\begin{aligned} & \left\{ X^{\text{TF}}[m, k], m = 0, \dots, N-1, k = 0, \dots, L-1 \right\} \rightarrow \\ & \rightarrow \left\{ X^{\text{TF}}[m, k'], m = 0, \dots, N-1, k' = 0, \dots, 2K-1 \right\}. \end{aligned} \quad (2)$$

Finally, the transmitted FBMC/OQAM-OTFS signal is generated by using the Heisenberg transformation [5, 6]:

$$s(t) = \sum_{m=0}^{N-1} \sum_{k'=0}^{2L-1} X^{\text{TF}}[m, k'] g^{\text{TX}}\left(t - \frac{k'T}{2}\right) \exp\left(j2\pi m \Delta f \left(t - \frac{k'T}{2}\right)\right), \quad (3)$$

where $g^{\text{TX}}(t)$ is the transmit prototype filter.

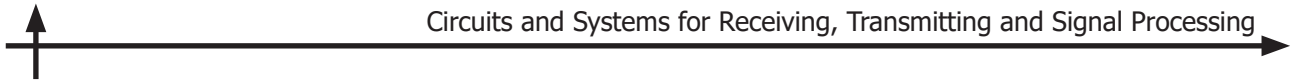
At the receiver, the time-domain signal without a noise component can be represented as follows [5, 6]:

$$r(t) = \int \int h(\tau, v) \exp(j2\pi v(t-\tau)) s(t-\tau) d\tau dv, \quad (4)$$

where $h(\tau, v)$ is the channel response in the DD domain which in turn can be represented as follows [5, 6]:

$$h(\tau, v) = \sum_{p=1}^P h_p \delta(t - \tau_p) \delta(v - v_p), \quad (5)$$

where h_p , τ_p , and v_p are the average path gain, path delay and path Doppler shift of the p -th path; and P is the number of signal propagation paths.



To detect information symbols in the TF domain, the matched filter and Wigner transformation are used [5, 6]:

$$G(\tau, v) = \int \exp(-j2\pi(t-\tau)) g^{\text{RX}}(t-\tau) r(t) dt; \quad (6)$$

$$Y^{\text{TF}}[l, k'] = G(\tau, v) \Big|_{\tau=k'T/2, v=m\Delta f}. \quad (7)$$

By applying OQAM post-processing, the QAM information symbols are taken as follows [5, 6]

$$\begin{aligned} \{Y^{\text{TF}}[m, k'], m = 0, \dots, N-1, k' = 0, \dots, 2L-1\} &\rightarrow \\ \rightarrow \{Y^{\text{TF}}[m, k], m = 0, \dots, N-1, k = 0, \dots, L-1\}. \end{aligned} \quad (8)$$

Then the received information symbols in the DD domain are obtained by using symplectic FFT (SFFT) as follows [5, 6]:

$$y^{\text{DD}}[n, l] = \frac{1}{\sqrt{NL}} \sum_{n=0}^{N-1} \sum_{l=0}^{L-1} Y^{\text{TF}}[m, k] \exp\left(-j2\pi\left(\frac{nm}{N} - \frac{lk}{L}\right)\right). \quad (9)$$

The Direct-FBMC/OQAM-OTFS modulation/demodulation incurs extremely high complexity due to the need for 2D transform calculations in [1, 9]. Therefore, this issue needs to be overcome before FBMC/OQAM-OTFS can be practically deployed in next-generation mobile networks.

In FBMC/OQAM-OTFS technique, the OTFS 2D-transformations add only a moderate computational load, whereas the FBMC/OQAM, which is a combination of 2D-transformations with the extended size and prototype filtering, dominates the overall complexity. Therefore, the focus here is on simplifying the FBMC/OQAM scheme.

FBMC/OQAM-OTFS implementation with frequency spreading

An alternative approach for implementing the FBMC/OQAM-OTFS modulation/demodulation is the frequency spreading technique (FS-FBMC/OQAM-OTFS) [7]. In this approach, the real and imaginary parts of the information symbols are processed in the frequency domain through an upsampling and filtering operation performed prior to the IFFT with an extended size. The structure of the FS-FBMC/OQAM-OTFS scheme is illustrated in Fig. 3.

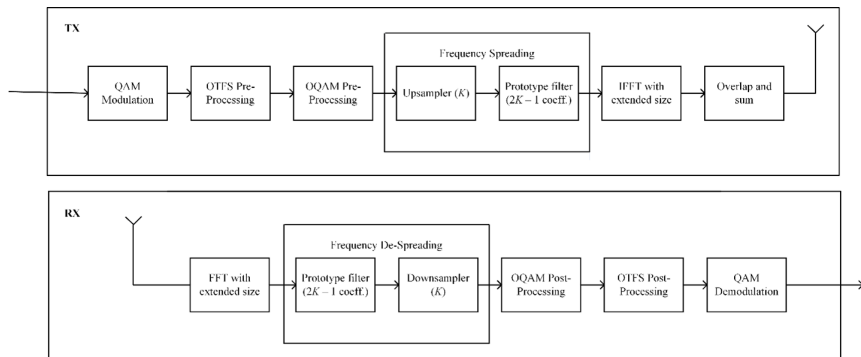


Fig. 3. FS-FBMC/OQAM-OTFS scheme

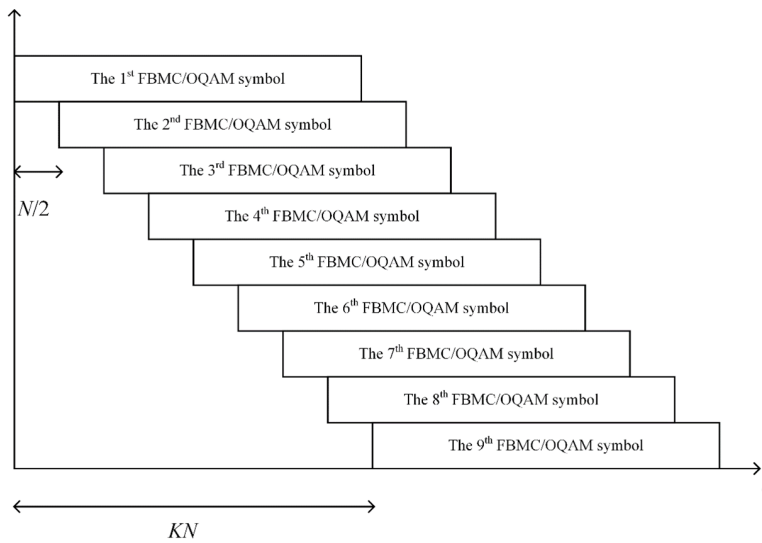


Fig. 4. Illustration of summing of overlapping FBMC/OQAM-OTFS symbols

At the transmitter, at the first stage, the OQAM pre-processing is used after ISFFT operation, where the in-phase and quadrature components of the QAM symbols are time-shifted by half the symbol duration. As a result, the orthogonality between subcarriers is preserved. After OQAM pre-processing, each OQAM symbol is upsampled by the overlapping factor of K and filtered by a prototype filter in the frequency domain. This combination of upsampling and filtering process constitutes the frequency spreading operation. Accordingly, the IFFT size is extended by a factor of K . As can be seen from Fig. 4, at the final stage, the transmitted signal is formed by summing of overlapping FS-FBMC/OQAM-OTFS symbols following each other with a step of $N/2$ samples. At the receiver, the received signal is processed in the reverse order of the transmitter operations, with the real and imaginary parts being handled separately.

Proposed low computational complexity FBMC/OQAM-OTFS implementation

The FS-FBMC/OQAM-OTFS technique is still ineffective in terms of the computational complexity due to the use of frequency spreading and FFT/IFFT operations with the size KN . Therefore, in this work, we propose two alternative implementation approaches for the FBMC/OQAM-OTFS technique based on a polyphase structure (PPN-FBMC/OQAM-OTFS).

The filters used for FBMC/OQAM-OTFS modulation are a finite impulse response (FIR) filters with the length $P = KN$. The relationship between the input and output of the filter is expressed as follows:

$$y[n] = \sum_{i=0}^{P-1} h_i x[n]. \quad (10)$$

Applying the Z -transformation to (10), we obtain

$$\begin{aligned} H(Z) &= \sum_{i=0}^{P-1} h[i] Z^{-i} = \sum_{n=0}^{N-1} \sum_{k=0}^{K-1} h[kN + n] Z^{-(kN+n)} = \\ &= \sum_{n=0}^{N-1} \left(\sum_{k=0}^{K-1} h[kN + n] Z^{-kN} \right) Z^{-n} = \sum_{n=0}^{N-1} E_n(Z^N) Z^{-n}, \end{aligned} \quad (11)$$

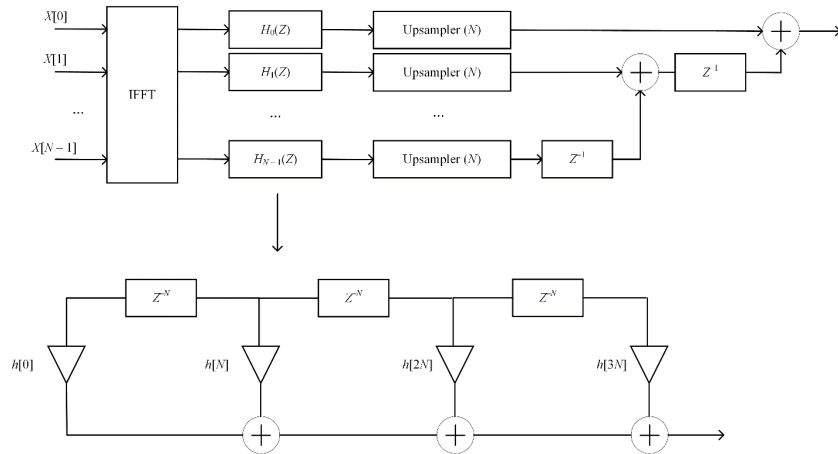


Fig. 5. Polyphase structure in PPN-FBMC/OQAM-OTFS transmitter

where $E_n(Z^N) = \sum_{k=0}^{K-1} h(kN+n)Z^{-kN}$ is the elementary component of the filter $H(Z)$. As seen from (11), the filter $H(Z)$ can be decomposed into N elementary components, as depicted in Fig. 5.

Consider a version of the $H_i(Z)$ filter, which is obtained by shifting of $H(Z)$ by i/N in the frequency domain. Using the polyphase representation, $H_i(Z)$ filter is defined as:

$$H_i(Z) = \sum_{i=0}^{P-1} h[i] e^{j2\pi i/N} Z^{-i} = \sum_{n=0}^{N-1} \sum_{k=0}^{K-1} h[kN+n] e^{j2\pi i(kN+n)/N} Z^{-(kN+n)} = \sum_{n=0}^{N-1} e^{j2\pi ni/N} E_n(Z^N) Z^{-n}. \quad (12)$$

Denote $W = \exp(-j2\pi/N)$. From (12), it follows that the filter bank is obtained by shifting $H(Z)$ in the frequency domain by a multiple of $1/N$ and is defined as follows:

$$\begin{bmatrix} H_0(Z) \\ H_1(Z) \\ \dots \\ H_{N-1}(Z) \end{bmatrix} = \begin{bmatrix} 1 & 1 & \dots & 1 \\ 1 & W^{-1} & \dots & W^{-(N-1)} \\ \dots \\ 1 & W^{-(N-1)} & \dots & W^{-(N-1)^2} \end{bmatrix} \begin{bmatrix} E_0(Z^N) \\ Z^{-1}E_1(Z^N) \\ \dots \\ Z^{-(N-1)}E_{N-1}(Z^N) \end{bmatrix}. \quad (13)$$

Obviously, matrix \mathbf{W} is the matrix of an IFFT operation. Accordingly, the corresponding filter bank structure at the transmitter side is illustrated in Fig. 6. At the receiver side, the filter bank corresponds to an FFT operation as described in (14), and its structure is also depicted in Fig. 6.

$$\begin{bmatrix} H_0(Z) \\ H_{-1}(Z) \\ \dots \\ H_{-(N-1)}(Z) \end{bmatrix} = \begin{bmatrix} 1 & 1 & \dots & 1 \\ 1 & W & \dots & W^{N-1} \\ \dots \\ 1 & W^{N-1} & \dots & W^{(N-1)^2} \end{bmatrix} \begin{bmatrix} E_0(Z^N) \\ Z^{-1}E_1(Z^N) \\ \dots \\ Z^{-(N-1)}E_{N-1}(Z^N) \end{bmatrix}. \quad (14)$$

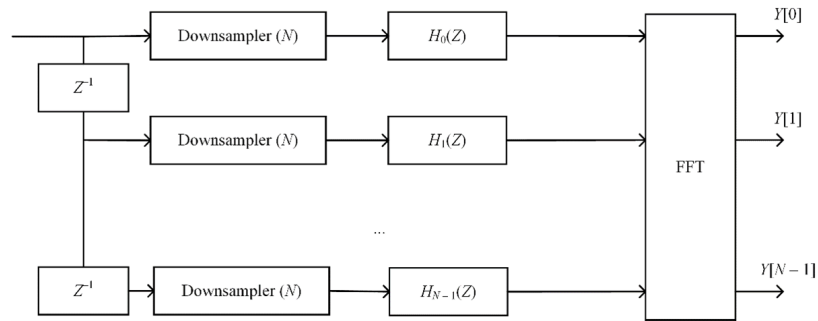


Fig. 6. Polyphase structure in PPN-FBMC/OQAM-OTFS receiver

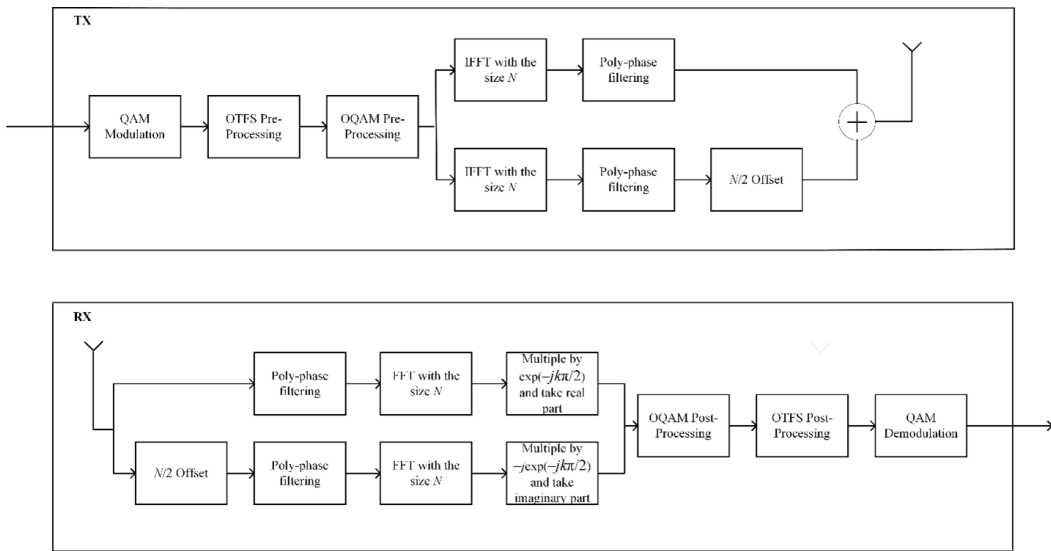


Fig. 7. PPN-FBMC/OQAM-OTFS scheme

Unlike the approach based on the frequency spreading, the PPN-FBMC/OQAM-OTFS technique uses only two FFT/IFFT operations with the size of N , thus significantly reducing computational complexity of the implementing the FBMC/OQAM-OTFS. The scheme of the PPN-FBMC/OQAM-OTFS technique is shown in Fig. 7.

This work also proposes an approach to further reduce the computational complexity of the PPN-FBMC/OQAM-OTFS transmitter, referred to as the low-complexity PPN-FBMC/OQAM-OTFS scheme. In this approach, complex information symbols are used instead of two OQAM symbols as the input of IFFT block, which reduces the cost of two N -IFFT operations to one N -IFFT operation with additional signal processing. To achieve this, the principle of computing the discrete inverse Fourier transforms of two real functions simultaneously using a single IFFT block, as described in [9], is utilized. The multiplication with the phase rotation from OQAM pre-processing in the frequency domain can be replaced by a circular shift of $N/4$ in time domain [10]. The scheme of low-complexity PPN-FBMC/OQAM-OTFS transmitter is shown in Fig. 8.

Computational complexity comparison

An important factor in the computational complexity analysis is the agreement about computational complexity of the multiplication of two complex numbers. Usually, it is used two common ways: either

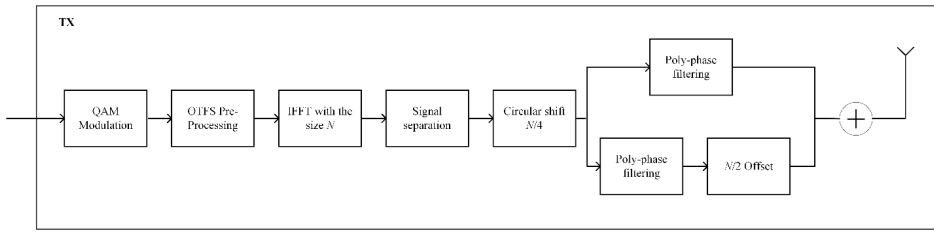


Fig. 8. Low-complexity PPN-FBMC/OQAM-OTFS transmitter

using three additions and three multiplications or using two additions and four multiplications of real numbers [7]. Since the cost of multiplication is significantly higher than that of addition [7], this work adopts the first method. Based on this assumption, the computational complexity of different considered modulation/demodulation techniques is summarized in Tables 1 and 2.

Table 1
Computational complexity comparison on the transmitter side

	Number of real multiplications	Number of real additions
OFDM Tx	$L(N(\log_2 N - 3) + 4)$	$L(3N(\log_2 N - 1) + 4)$
OTFS Tx	$3L(N(\log_2 N - 3) + 4)$	$3L(3N(\log_2 N - 1) + 4)$
Direct-FBMC/OQAM Tx	$6LN^2K^2 + 4LN(K - 1)$	$6LN^2K^2 + N(2K - 1)(2L - 1)$
FS-FBMC/OQAM Tx	$2L(NK(\log_2 NK - 3) + 4 + 2N(K - 1))$	$2L(3NK(\log_2 NK - 1) + 4) + 2N(K - 1)(2L - 1)$
PPN-FBMC/OQAM Tx	$2L(2NK + N(\log_2 N - 3) + 4)$	$2L(3N(\log_2 N - 1) + 4 + 2N(K - 1) + 2N(L + K - 2))$
Low-complexity PPN-FBMC/OQAM Tx	$L(N(\log_2 N - 3) + 4 + 4NK)$	$L(3N(\log_2 N - 1) + 4 + 4N(K - 1) + 4N) + 2N(L + K - 2)$
Direct-FBMC/OQAM-OTFS Tx	$6LN^2(1 + K^2) + 4LN(K - 1)$	$6LN^2(1 + K^2) + N(2K - 1)(2L - 1)$
FS-FBMC/OQAM-OTFS Tx	$2L(N(\log_2 N - 3) + 4) + 2L(NK(\log_2 NK - 3) + 4 + 2N(K - 1))$	$2L(3N(\log_2 N - 1) + 4) + 2L(3NK(\log_2 NK - 1) + 4) + 2N(K - 1)(2L - 1)$
PPN-FBMC/OQAM-OTFS Tx	$2L(N(\log_2 N - 3) + 4) + 2L(2NK + (N(\log_2 N - 3) + 4))$	$2L(3N(\log_2 N - 1) + 4) + 2L(3N(\log_2 N - 1) + 4 + 2N(K - 1)) + 2N(L + K - 2)$
Low-complexity PPN-FBMC/OQAM-OTFS Tx	$2L(N(\log_2 N - 3) + 4) + L(N(\log_2 N - 3) + 4 + 4NK)$	$2L(3N(\log_2 N - 1) + 4) + L(3L(\log_2 N - 1) + 4 + 4N(K - 1) + 4N) + 2N(L + K - 2)$

Tables 1 and 2 show the dependences of the number of required operations on the values of N_{FFT} (in Tables 1 and 2 it is marked as N to abbreviate notation), L and K . It is clear that the FS and PPN approaches allow us to reduce the required costs, but it is difficult to draw an exact conclusion. Therefore, Table 3 provides a comparison of the computational complexity of various modulation techniques in terms of the number of real multiplications and additions for $N_{\text{FFT}} = 256$, $L = 20$, and $K = 4$. The results indicate that the computational complexity of OTFS modulation/demodulation is three times higher than that of OFDM for both real multiplications and additions. Regarding FBMC/OQAM techniques, the direct methods (Direct-FBMC/OQAM and Direct-FBMC/OQAM-OTFS) exhibit extremely high computational costs, requiring 4902.3 and 5208.6 times more real multiplications and 1169.4 and 1242.5 times more real additions, respectively, compared to OFDM. By contrast, the FS-FBMC/OQAM and FS-FBMC/OQAM-OTFS schemes substantially reduce computational complexity relative to the direct methods but still demand 13.6–15.6 times more real multiplications and

10.9–12.9 times more real additions than for OFDM, remaining considerably higher number of computations than both OFDM and OTFS. Notably, approaches based on the polyphase network (PPN-FBMC/OQAM and PPN-FBMC/OQAM-OTFS), along with their simplified versions, achieve significant reductions in computational complexity, requiring only 1.4–7.2 times more operations than for OFDM. In particular, the low-complexity PPN-FBMC/OQAM-OTFS scheme requires only 6.2 times more real multiplications and 3.4 times more real additions than OFDM.

Table 2
Computational complexity comparison on the receiver side

	Number of real multiplications	Number of real additions
OFDM Rx	$L(N(\log_2 N - 3) + 4)$	$L(3N(\log_2 N - 1) + 4)$
OTFS Rx	$3L(N(\log_2 N - 3) + 4)$	$3L(3N(\log_2 N - 1) + 4)$
Direct-FBMC/OQAM Rx	$6LN^2K^2 + 4LN(K - 1)$	$6LN^2K^2$
FS-FBMC/OQAM Rx	$2L(NK(\log_2 NK - 3) + 4 + 2N(K - 1))$	$2L(3NK(\log_2 NK - 1) + 4) + 2N(K - 1)(2L - 1)$
PPN-FBMC/OQAM Rx	$2L(2NK + N(\log_2 N - 3) + 4)$	$2L(3N(\log_2 N - 1) + 4 + 2N(K - 1) + 2N(L + K - 2))$
Low-complexity PPN-FBMC/OQAM Rx	$L(N(\log_2 N - 3) + 4 + 4NK)$	$L(3N(\log_2 N - 1) + 4 + 2N(K - 1) + 2N(L + K - 2))$
Direct-FBMC/OQAM-OTFS Rx	$6LN^2(1 + K^2) + 4LN(K - 1)$	$6LN^2(1 + K^2)$
FS-FBMC/OQAM-OTFS Rx	$2L(N(\log_2 N - 3) + 4) + 2L(NK(\log_2 NK - 3) + 4 + 2N(K - 1))$	$2L(3N(\log_2 N - 1) + 4) + 2L(3NK(\log_2 NK - 1) + 4) + 2N(K - 1)(2L - 1)$
PPN-FBMC/OQAM-OTFS Rx	$2L(N(\log_2 N - 3) + 4) + 2L(2NK + (N(\log_2 N - 3) + 4))$	$2L(3N(\log_2 N - 1) + 4) + 2L(3N(\log_2 N - 1) + 4 + 2N(K - 1)) + 2N(L + K - 2)$
Low-complexity PPN-FBMC/OQAM-OTFS Rx	$2L(N(\log_2 N - 3) + 4) + L(N(\log_2 N - 3) + 4 + 4NK)$	$2L(3N(\log_2 N - 1) + 4) + L(3N(\log_2 N - 1) + 4 + 2N(K - 1)) + 2N(L + K - 2)$

Table 3
Computational complexity comparison for the case of $N = 256$, $L = 20$, and $K = 4$

	Number of real multiplications divided by such a value for OFDM	Number of real additions divided by such a value for OFDM
OFDM	1	1
OTFS	3	3
Direct-FBMC/OQAM	4902.3	1169.4
FS-FBMC/OQAM	13.6	10.9
PPN-FBMC/OQAM	5.2	2.6
Low-complexity PPN-FBMC/OQAM	4.2	1.4
Direct FBMC/OQAM-OTFS	5208.6	1242.5
FS-FBMC/OQAM-OTFS	15.6	12.9
PPN-FBMC/OQAM-OTFS	7.2	4.6
Low-complexity PPN-FBMC/OQAM-OTFS	6.2	3.4

Simulation results and discussion

The simulation parameters are summarized in Table 4.

Table 4
Simulation parameters

Parameters	Value
Modulation technique	CP-OFDM, OTFS, FBMC/OQAM, Direct-FBMC/OQAM-OTFS, FS-FBMC/OQAM-OTFS, PPN-FBMC/OQAM-OTFS, low-complexity FBMC/OQAM-OTFS
N_{FFT}	256
Number of active subcarriers, M	200
Number of symbols, N	20
Length of cyclic prefix in samples (for CP-OFDM)	20
Modulation	QPSK
Equalization method	LMMSE
FEC	LDPC with code rate 1/2
Prototype filter	Phydyas
FBMC/OQAM overlapping factor, K	4
Channel model	EPA/EVA/ETU
Maximal Doppler shift (Hz)	5 – 3000

Shapes of signal spectrum

Spectrum shapes of different modulations are shown in Fig. 9. According to it, all combinations of modulations are divided into two groups: containing and not containing FBMC. That is the first group includes OFDM, OTFS signals, and the second group includes Direct FBMC/OQAM, Direct-FBMC/OQAM-OTFS, FS-FBMC/OQAM-OTFS, PPN-FBMC/OQAM-OTFS and low-complexity PPN-FBMC/OQAM-OTFS signals. Spectrums of each group are almost the same. Modulations containing FBMC provide up to about 100 dB lower level of OOB with respect to others. Further reduction of the OOB level can be achieved by applying a higher value of K .

BER Performance

Fig. 10 shows the BER performance of OFDM, OTFS and FBMC/OQAM-OTFS signals under the EVA channel model at Doppler shifts of 70 and 700 Hz, assuming perfect channel estimation. As illustrated, the Direct-FBMC/OQAM-OTFS, FS-FBMC/OQAM-OTFS and OTFS signals exhibit identical BER performance, while the PPN-FBMC/OQAM-OTFS and low-complexity PPN-FBMC/OQAM-OTFS signals likewise achieve the same BER performance. Direct-FBMC/OQAM-OTFS, FS-FBMC/OQAM-OTFS and OTFS signals provide energy gain with respect to CP-OFDM signal, about 1.52 and 1.35 dB at the $BER = 10^{-4}$ for the Doppler shifts of 70 and 700 Hz, respectively. Meanwhile, using PPN-FBMC/OQAM-OTFS and low-complexity PPN-FBMC/OQAM-OTFS signals provides an energy loss of only about 0.81 and 0.67 dB compared to the OTFS, Direct-FBMC/OQAM-OTFS and FS-FBMC/OQAM-OTFS signals for the Doppler shifts of 70 and 700 Hz, respectively. It can be explained that the frequency spreading implementation allows for a more accurate control of the filter bank's frequency response by manipulating each subcarrier individually in the frequency domain. This leads to improvement suppression of ICI compared to the conventional PPN implementation¹ [11].

¹ Prototype filter and structure optimization, Available: <http://www.ict-phydyas.org/delivrables/PHYDYAS-D5.1.pdf> (Accessed 04.12.2025)

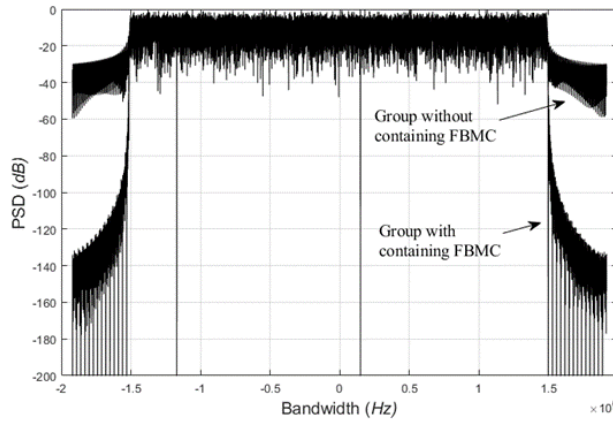


Fig. 9. Spectrum shapes of OFDM, OTFS, FBMC and their combinations. $N_{\text{FFT}} = 256$ and the number of active subcarriers $M = 200$. For FBMC Phydys filter is used and $K = 4$

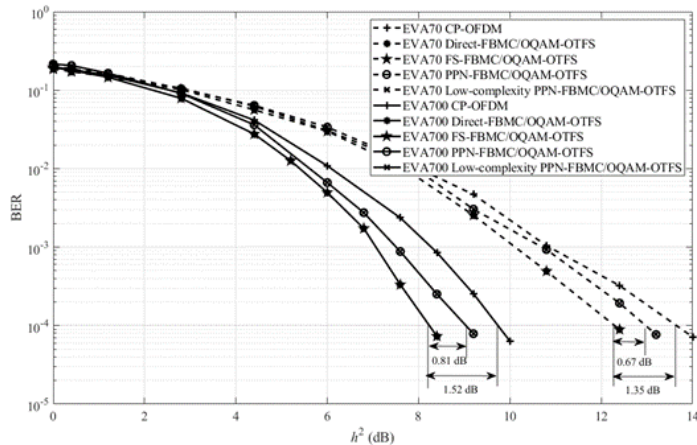


Fig. 10. BER performance over EVA 70/700 Hz of different modulation techniques

Table 5 shows the values of h^2 of mentioned modulation techniques at the $\text{BER} = 10^{-4}$ for different multipath channel profiles EPA, EVA and ETU from moderate to highly dynamic scenarios. From Table 5 it follows that the relative positions of the BER curves in Fig. 10 remain the same, only the absolute values of h^2 change. For PPN-FBMC/OQAM-OTFS and low-complexity PPN-FBMC/OQAM-OTFS signals, the energy losses are approximately about 0.57, 0.62, 0.68, 0.8, 0.41 and 0.95 dB compared to Direct-FBMC/OQAM-OTFS and FS-FBMC/OQAM-OTFS signals in EPA5, EPA500, EVA70, EVA700, ETU300 and ETU3000, respectively. For CP-OFDM signal, the energy losses are approximately about 1.12, 1.22, 3.36, 1.51 and 3.16 compared to Direct-FBMC/OQAM-OTFS and FS-FBMC/OQAM-OTFS signals in EPA5, EPA500, EVA70, EVA700 and ETU300, respectively. CP-OFDM signal is not reached $\text{BER} = 10^{-4}$ even on the noise-free channel, $h^2 = \text{inf}$.

Table 5

The energy cost of modulation techniques at the $BER = 10^{-4}$

	Direct-FBMC/ OQAM-OTFS	FS-FBMC/ OQAM-OTFS*	PPN-FBMC/ OQAM-OTFS*	Low-complexity PPN-FBMC/ OQAM-OTFS*	CP-OFDM*
EPA5	22.63	0	0.57	0.57	1.12
EPA500	14.25	0	0.62	0.62	1.22
EVA70	12.29	0	0.68	0.68	1.35
EVA700	8.23	0	0.8	0.8	1.52
ETU300	7.19	0	0.41	0.41	3.16
ETU3000	9.98	0	0.95	0.95	—**

* The energy loss relative to Direct-FBMC/OQAM-OTFS at $BER = 10^{-4}$.

** $BER = 10^{-4}$ is not reached even on the noise-free channel, $h^2 = \text{inf}$.

Conclusion

This paper introduces a low-complexity FBMC/OQAM-OTFS scheme based on a polyphase structure (PPN-FBMC/OQAM-OTFS) for future wireless communication systems. Simulation results demonstrate that the proposed PPN-FBMC/OQAM-OTFS approaches achieve a reduction in computational complexity about 2.5–4 times, with an energy loss of no more than 1 dB under various channel models with different maximum Doppler shifts, when compared to the FS-FBMC/OQAM-OTFS technique. These findings suggest that the PPN-FBMC/OQAM-OTFS technique is a feasible and promising alternative to conventional OFDM in high-mobility wireless scenarios.

REFERENCES

1. **Hadani R., Rakib S., Tsatsanis M., Monk A., Goldsmith A.J., Molisch A.F.** Orthogonal time frequency space modulation. *2017 IEEE Wireless Communications and Networking Conference (WCNC)*, 2017, Pp. 1–6. DOI: 10.1109/WCNC.2017.7925924
2. **He X., Fan P., Wang Q.** A two-stage channel estimation algorithm for OTFS in fractional doppler channels. *IEEE Communications Letters*, 2023, Vol. 27, No. 7, Pp. 1839–1843. DOI: 10.1109/LCOMM.2023.3270296
3. **Nguyen P.T.H., Khuc B., Petrov I., Lavrukhin T., Gelgor A.** Improvement in data transmission efficiency in mobile 5G new radio system using filter bank multicarrier signals. *2022 International Conference on Electrical Engineering and Photonics (EExPolytech)*, 2022, Pp. 63–66. DOI: 10.1109/EExPolytech56308.2022.9950816
4. **Hammodi A., Audah L., Taher M.A.** Green coexistence for 5G waveform candidates: A review. *IEEE Access*, 2019, Vol. 7, Pp. 10103–10126. DOI: 10.1109/ACCESS.2019.2891312
5. **Khuc B., Gelgor A., Le Duc T., Nguyen P.T.H.** FBMC/OQAM with OTFS pre-processing for high-mobility channels. *2024 International Conference on Electrical Engineering and Photonics (EExPolytech)*, 2024, Pp. 186–189. DOI: 10.1109/EExPolytech62224.2024.10755876
6. **Pereira Junior R., da Rocha C.A.F., Chang B.S., Le Ruyet D.** A two-dimensional FFT precoded filter bank scheme. *IEEE Transactions on Wireless Communications*, 2023, Vol. 22, No. 11, Pp. 8366–8377. DOI: 10.1109/TWC.2023.3262442
7. **Husam A.-A., Kollár Z.** Complexity comparison of filter bank multicarrier transmitter schemes. *2018 11th International Symposium on Communication Systems, Networks & Digital Signal Processing (CSNDSP)*, 2018, Pp. 1–4. DOI: 10.1109/CSNDSP.2018.8471795

8. **Mattera D., Tanda M., Bellanger M.** Analysis of an FBMC/OQAM scheme for asynchronous access in wireless communications. *EURASIP Journal on Advances in Signal Processing*, 2015, Vol. 23, Pp. 1–22. DOI: 10.1186/s13634-015-0191-4
9. **Brigham E.O.** *The fast Fourier transform and its applications*. New Jersey: Prentice Hall Inc., 1974.
10. **Varga L., Kollár Z.** Low complexity FBMC transceiver for FPGA implementation. *2013 23rd International Conference Radioelektronika (RADIOELEKTRONIKA)*, 2013, Pp. 219–223. DOI: 10.1109/RadioEl-ek.2013.6530920
11. **Vo-Huu T., Ludant N., Vo-Huu T., Noubir G.** Pilotless FS-FBMC for flexible spectrum access and sharing. *2021 IEEE International Symposium on Dynamic Spectrum Access Networks (DySPAN)*, 2021, Pp. 193–202. DOI: 10.1109/DySPAN53946.2021.9677265

INFORMATION ABOUT AUTHORS / СВЕДЕНИЯ ОБ АВТОРАХ

Bang Thanh Khuc
Хук Тхань Банг
E-mail: khucbang@mail.ru

Aleksandr L. Gelgor
Гельгор Александр Леонидович
E-mail: agelgor@spbstu.ru

Submitted: 22.09.2025; Approved: 20.11.2025; Accepted: 13.12.2025.
Поступила: 22.09.2025; Одобрена: 20.11.2025; Принята: 13.12.2025.